Synthesis of *C*-Linked Triazole-Containing AFGP Analogues and Their Ability to Inhibit Ice Recrystallization

Chantelle J. Capicciotti, John F. Trant, Mathieu Leclère, and Robert N. Ben*

Department of Chemistry, D'Iorio Hall, 10 Marie Curie, University of Ottawa, Ottawa, Ontario, Canada, K1N 6N5.

S *Supporting Information*

ABSTRACT: *C*-Linked antifreeze glycoprotein (*C*-AFGP) analogues have been shown to have potent ice recrystallization inhibition (IRI) activity. However, the lengthy synthesis of these compounds is not amenable to large-scale preparation for the many commercial, industrial, and medical applications that exist. This paper describes the synthesis of triazole-containing AFGPs using a convergent solid-phase synthesis (SPS) approach in which multiple carbohydrate derivatives are coupled to a resin-bound synthetic peptide in a single step. Modified "Click" conditions using dry DMF as solvent with catalytic Cu(II), sodium ascorbate, and microwave radiation afforded the synthesis of AFGP analogues **9**−**12** in 16−54% isolated yield. Compound **9** demonstrated no IRI activity, while compounds **10**, **11**, and **12** were moderate inhibitors of ice recrystallization. These results suggest that, while the triazole group is a structural mimetic of an amide bond, the amide bond in *C*-AFGP analogue **3** is an essential structural feature necessary for potent IRI activity.
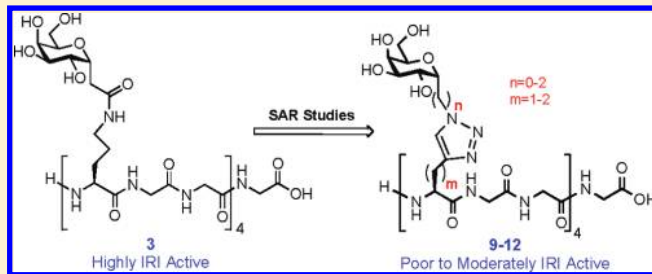
INTRODUCTION

Antifreeze glycoproteins (AFGPs) are found in many deep sea Teleost fish and serve to protect these organisms against cryo-injury and death. This is accomplished by inhibiting the growth of ice crystals *in vivo*—a phenomenon referred to as thermal hysteresis (TH). AFGPs are also potent inhibitors of ice recrystallization, and it has been recently hypothesized that this property would be beneficial for a cryoprotectant.[1] Cryopreservation experiments have been performed with AFGPs, but thermal hysteresis activity has been shown to cause significant cellular damage at temperatures below the thermal hysteretic gap,[2,3] thus ensuring that these compounds will not be further developed as cryoprotectants. However, AFGP analogues possessing "custom-tailored antifreeze activity" (i.e., are potent inhibitors of ice recrystallization but do not possess TH activity) have great potential as cryoprotectants that is presently unrealized.

During the past decade, our lab has been actively designing and synthesizing *C*-linked analogues of the native AFGP (*C*-AFGPs) in an effort to better understand their interactions at the ice—bulk water interface. Towards this end, we have reported the synthesis of several *C*-AFGP analogues (e.g., **3** and **5**) that exhibit potent ice recrystallization inhibition (IRI) activity but display no TH activity and have tremendous potential as novel cryoprotectants (Figure 1).[4,5] Structure—function studies on these *C*-AFGPs have questioned the functional importance of the amide bond in **3** for IRI activity. For instance, when the amide bond is removed as in *C*-serine analogue **5**, IRI activity is retained.[5] In contrast, other studies have shown that activity is significantly decreased when the length of the amide

bond-containing side chain in **3** was either lengthened or shortened (Figure 1).[6] Molecular dynamics (MD) simulations and variable temperature (VT) NMR experiments suggest that the IRI activity of **3** is attributed to an unusual conformation in which the carbohydrate moiety folds back over the peptide chain creating a hydrophobic pocket. It was hypothesized that this "pocket" disrupts the ordering of water molecules in the primary hydration shell of the galactose moiety, resulting in IRI activity.[6] However, it is not known whether the amide bond in these analogues is an important structural feature necessary for this activity. One manner in which to probe the importance of this linkage is to utilize a suitable isostere. The 1,4-disubstituted triazole has been shown by Wong and co-workers to be an isostere of a *Z*-amide bond (Figure 2).[7,8] Furthermore, the mild, highly efficient copper-catalyzed Huisgen cycloaddition for the preparation of triazoles has facilitated their use in many biologically significant molecules.[9−19]

Prior syntheses of *C*-AFGPs by our laboratory have utilized a traditional linear synthesis requiring the preparation of a glycosylated amino acid prior to solid-phase synthesis (SPS). This approach can be lengthy and expensive.[20,21] Alternatively, convergent methodologies have been reported for the synthesis of glycoconjugates in which several carbohydrates are simultaneously coupled to the resin-bound peptide.[22−24] Two convergent syntheses of triazole-containing AFGP analogues have been reported. A triazole-containing proline AFGP analogue was
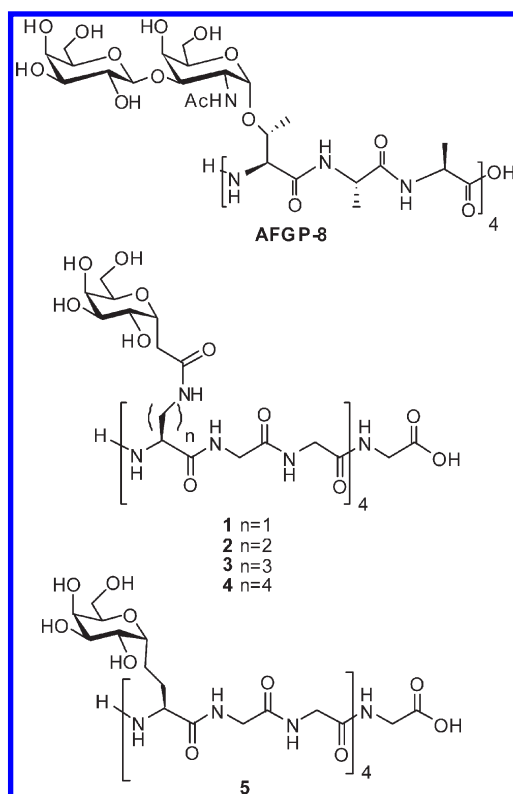
Figure 1. Previously prepared C-linked *C*-AFGP analogues.

Figure 2. Electronic similarities between a Z-amide bond and a 1,4-disubstituted triazole ring.

synthesized in a solution-phase approach through coupling of an acetylenic carbohydrate derivative and an azido peptide using 10−20% CuSO$_4$ and 25−50% sodium ascorbate at 80 °C in the presence of microwaves.[25] In another approach, three AFGP peptoids (**6**, **7**, and **8**, shown in Figure 3) were prepared by coupling azido sugars with a resin-bound acetylenic peptoid using excess CuI and sodium ascorbate in anhydrous DMF and DIPEA.[26] On the basis of this precedent, we sought to prepare triazole-containing AFGP analogues of **3** using "Click" chemistry in a convergent solid-phase approach. The structures of these analogues (**9−12**) are shown in Figure 4. The goal of this study is to understand the functional importance of the amide bond in the side chain of *C*-AFGP analogue **3**.

■ EXPERIMENTAL PROCEDURES

General Methods and Materials. All anhydrous reactions were performed in flame-dried glassware under a positive pressure of dry argon. Air- or moisture-sensitive reagents and anhydrous solvents were transferred with oven-dried syringes or cannulae. All flash chromatography was performed with E. Merck silica gel 60 (230−400 mesh). All solution-phase reactions were monitored using analytical thin layer chromatography (TLC) with 0.2 mm precoated silica gel aluminum plates 60 F254 (E. Merck). Components were visualized by illumination with a short-wavelength (254 nm) ultraviolet light and/or staining (ceric ammonium molybdate, potassium permanganate, or orcinol stain solution). Dry-vacuum chromatography was carried out according to the protocol outlined by Pedersen and Rosenbohm.[27] All solvents used for anhydrous reactions were distilled. Tetrahydrofuran (THF) was distilled from sodium/benzophenone under nitrogen. Dichloromethane (DCM), triethylamine,
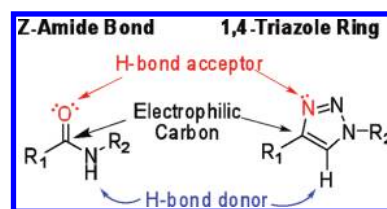
and diisopropylethylamine (DIPEA) were distilled from calcium hydride. *N,N*-Dimethylformamide (DMF) was stored over activated 4 Å molecular sieves under argon. ^{1}H (400 or 500 MHz) and ^{13}C NMR (100 or 125 MHz) spectra were recorded at ambient temperature on a Bruker Avance 400, Bruker Avance 500, or Varian Inova 500 spectrometer. Deuterated chloroform (CDCl$_3$), methanol (CD$_3$OD), or water (D$_2$O) were used as NMR solvents. Chemical shifts are reported in ppm downfield from trimethylsilane (TMS) or the solvent residual peak as an internal standard. Splitting patterns are designated as follows: s, singlet; d, doublet; t, triplet; q, quartet; m, multiplet; and br, broad. Low resolution mass spectrometry (LRMS) was performed on a Micromass Quatro-LC Electrospray spectrometer with a pump rate of 20 μL/min using electrospray ionization (ESI), a Voyager DE-Pro matrix-assisted laser desorption/ionization-time-of-flight (MALDI-TOF) (Applied Biosystem, Foster City, CA) mass spectrometer operated in the reflectron/positive-ion mode with DHB in 20% EtOH/H$_2$O as the MALDI matrix, or a Bruker Microflex MALDI-TOF mass spectrometer with DHB in 20% acetonitrile/H$_2$O as the MALDI matrix. Analytical and preparatory scale RP-HPLC were carried out with Varian Polaris C-18 columns on a Varian Prostar HPLC system equipped with a variable wavelength detector (ProStar 330 PDA). Desalting was accomplished using C18 solid-phase extraction cartridges (Discovery, Supelco) using 40% acetonitrile in water for elution of glycopeptides. All yields are unoptimized.

Circular Dichroism. CD spectra of the glycopolymers **9−12** were obtained using a Jasco model *J*-810 automatic recorder spectropolarimeter interfaced with a Dell computer. All of the measurements were performed in quartz cells with 1.0 cm path length. Spectra were obtained with a 1.0 nm bandwidth, a time constant of 2 s, and a scan speed of 50 nm/min. Eight scans were added to improve the signal-to-noise ratio, and baseline corrections were made against each sample. All of the spectra were recorded between 190 and 300 nm, and all of the CD experiments were performed in doubly distilled H$_2$O at pH 7.4. Data obtained from CD spectroscopy were converted into molar ellipticities (deg cm^2 dmol^{-1}). Glycopeptide secondary structures were estimated using the deconvolution software *CD Pro*. The data from each spectrum were analyzed using three different deconvolution programs: SELCON3, CDSSTR, and CONTINLL. Of these three programs, SELCON3 and CONTINLL gave the most consistent results. IBASIS 5 was used as the set of reference proteins; it contains 37 proteins with α-helix, β-structure, polyproline II, and unordered conformations with optimal wavelengths of 185−240 nm.[6]

Thermal Hysteresis (TH) Assay. Nanoliter osmometry was performed using a Clifton nanoliter osmometer (Clifton Technical Physics, Hartford, NY), as described by Chakrabartty and Hew.[28] All of the measurements were performed in doubly distilled water. Ice crystal morphology was observed through a
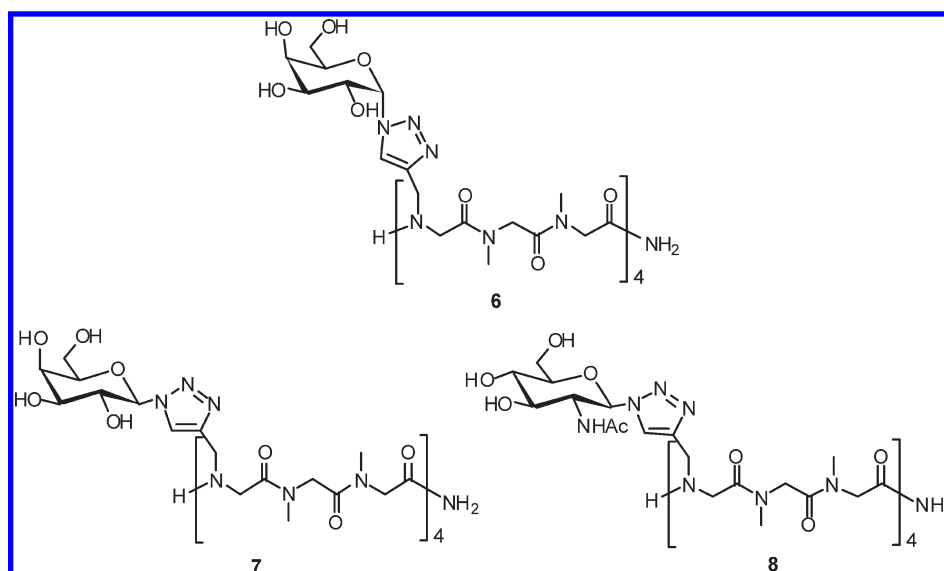
Figure 3. Triazole-containing peptoid analogues synthesized by Norgren et al.
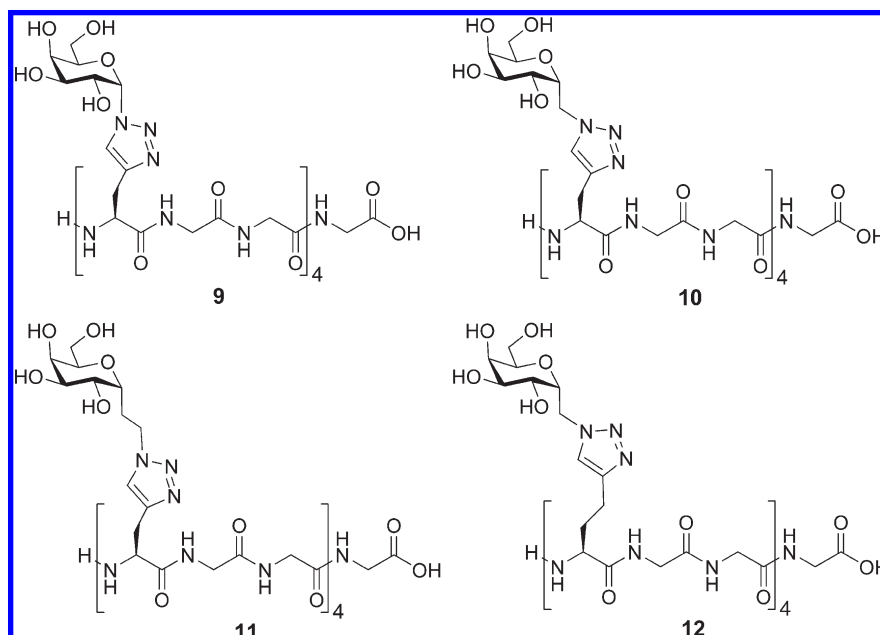
Figure 4. Proposed structures of triazole-containing AFGP analogues.

Leitz compound microscope equipped with an Olympus 20× (infinity-corrected) objective, a Leitz Periplan 32× photo eyepiece, and a Hitachi KPM2U CCD camera connected to a Toshiba MV13K1 TV/VCR system. Still images were captured directly using a Nikon CoolPix digital camera.

Ice Recrystallization Inhibition (IRI) Assay. Sample analysis for IRI activity was performed using the "splat cooling" method as previously described.[1] In this method, the analyte was dissolved in phosphate buffered saline (PBS) solution and a 10 μL droplet of this solution was dropped from a micropipet through a 2-m-high plastic tube (10 cm in diameter) onto a block of polished aluminum precooled to approximately −80 °C. The droplet froze instantly on the polished aluminum block and was approximately 1 cm in diameter and 20 μm thick. This wafer was then carefully removed from the surface of the block and transferred to a cryostage held at −6.4 °C for annealing. After a period of 30 min, the wafer was photographed between crossed polarizing filters using a digital camera (Nikon CoolPix 5000) fitted to the microscope. A total of three images were taken from each wafer. During flash freezing, ice crystals spontaneously nucleated from the supercooled solution. These initial crystals were relatively homogeneous in size and quite small. During the annealing cycle, recrystallization occurred, resulting in a dramatic increase in ice crystal size. A quantitative measure of the difference in recrystallization inhibition of two compounds X and Y is the difference in the dynamics of the ice crystal size distribution. Image analysis of the ice wafers was performed using a novel domain recognition software (DRS) program.[29]

This processing employed the Microsoft Windows Graphical User Interface to allow a user to visually demarcate and store the vertices of ice domains in a digital micrograph. The data was then used to calculate the domain areas. All data was plotted and analyzed using Microsoft *Excel*. IRI activity is reported as a ratio of the mean grain size (MGS) of ice crystals in the presence of the solute divided by the mean grain size (MGS) of ice crystals in a control solution of phosphate buffered saline (PBS). Small ratios indicate high levels of ice recrystallization inhibition.

N-[[(9*H*-Fluoren-9-ylmethoxy)carbonyl]amino]-L-propargylglycine allyl ester (13). In a flame-dried round-bottom flask with 4 Å molecular sieves, Fmoc-L-Propargylglycine (338 mg, 1.01 mmol) was dissolved in anhydrous DCM (7 mL) under argon atmosphere. HBTU (460 mg, 1.2 mmol) was added and the mixture was stirred for 20 min. Allyl alcohol (347 μL, 5.1 mmol) was added, followed by a dropwise addition of DIPEA (355.5 μL, 2.04 mmol). The reaction was stirred at room temperature for 16 h. Upon consumption of starting material, the reaction was diluted with DCM, filtered through a Celite pad, and washed with 10% HCl, NaHCO$_3$, and brine successively. The final product was purified by dry vacuum chromatography (DVC) to yield 326 mg of a white powder (86% yield). ^{1}H NMR (400 MHz, CDCl$_3$): δ_{ppm} 7.77 (d, 2H, J = 7.5 Hz), 7.61 (d, 2H J = 7.4 Hz), 7.40 (t, 2H, J = 7.5 Hz), 7.32 (ddd, 2H, J = 7.5, 4.3, 1.1 Hz), 5.92 (ddd, 1H, J = 16.4, 10.8, 5.6 Hz), 5.66 (d, 1H, J = 8.1 Hz), 5.36 (dd, 1H, J = 17.2, 0.8 Hz), 5.28 (dd, 1H, J = 10.4, 0.9 Hz), 4.70 (dd, 2H, J = 2.7, 1.3 Hz), 4.61−4.54 (m, 1H), 4.40 (d, 2H, J = 7.2 Hz), 4.25 (t, 1H, J = 7.2 Hz), 2.82 (dd, 2H, J = 4.5, 2.6 Hz), 2.08 (t, 1H, J = 2.4 Hz). ^{13}C NMR (100 MHz, CDCl$_3$): δ_{ppm} 170.0, 155.6, 143.8, 143.7, 141.3, 131.3, 127.7, 127.1, 125.1, 120.0, 119.0, 72.0, 67.3, 66.4, 52.4, 47.1, 22.8. ESI-MS m/z calcd for C$_{23}$H$_{21}$NO$_4$ [M+H]$^+$: 376.154; [M+Na]$^+$: 398.137. Found: 376.14, 398.12.

2,3,4,6-Tetra-*O*-acetyl-α-D-galactopyranosyl Azide (14). 2,3,4,6-Tetra-*O*-acetyl-*β*-D-galactopyranosyl chloride[30] (4.68 g, 12.8 mmol) was dissolved in 15 mL of HMPA. Sodium azide (2.5 g, 38.4 mmol) was added and the reaction was stirred vigorously for 16 h at ambient temperature. The mixture was poured into an ice−water mixture and the solid was collected by filtration and washed with water. The product was recrystallized from ether and petroleum ether to yield 4.3 g of white crystals (89% yield). Characterization data are consistent with that reported previously in the literature.[31] ^{1}H NMR (400 MHz, CDCl$_3$): δ_{ppm} 5.67 (d, 1H, J = 3.9 Hz), 5.46 (dd, 1H J = 2.9, 1.2 Hz), 5.25 (dd, 1H, J = 10.8, 3.0 Hz), 5.20 (dd, 1H, J = 10.8, 3.9 Hz), 4.37 (dd, 1H, J = 6.5, 6.5 Hz), 4.12 (dd, 2H, J = 6.5, 4.4 Hz), 2.15 (s, 3H), 2.11 (s, 3H), 2.06 (s, 3H), 2.00 (s, 3H). ^{13}C NMR (100 MHz, CDCl$_3$): δ_{ppm} 170.4, 170.1, 170.0, 169.8, 86.7, 68.6, 67.6, 67.4, 67.2, 61.5, 20.67, 20.64, 20.60, 20.5. ESI-MS m/z calcd for C$_{14}$H$_{20}$N$_3$O$_9$ [M+H]$^+$: 374.12; [M+Na]$^+$: 396.10. Found: 374.09, 396.02.

1-Azido-2-(2,3,4,6-tetra-*O*-acetyl-α-D-galactopyranosyl) ethane (16). 2-(2,3,4,6-Tetra-*O*-acetyl-α-D-galactopyranosyl) acetaldehyde[5] (2.5 g, 6.7 mmol) was added to a round-bottom flask purged with argon and cooled to 0 °C. 70 mL of MeOH was then added followed by sodium borohydride (983 mg, 26 mmol) and the reaction was stirred for 40 min when TLC (1:1 hexanes:ethyl acetate) analysis showed consumption of starting material. The reaction was then quenched with 4 mL of acetic acid and the solvent was removed *in vacuo*. Following evaporation, the product was dissolved in ethyl acetate and

washed successively with 10% HCl, sodium bicarbonate, and brine to yield 2.6 g of crude oil. The product was sufficiently pure to be used directly in the next transformation.

A round-bottom flask was cooled to 0 °C in an ice bath. Crude 2-(2,3,4,6-tetra-*O*-acetyl-α-D-galactopyranosyl)ethanol (2.6 g, 6.7 mmol) and methanesulfonylchloride (2.1 mL, 26.8 mmol) were then added to the flask and dissolved in 33 mL of pyridine (0.2 M). The reaction was stirred at 0 °C for 1.5 h. Once complete, the reaction was diluted with ethyl acetate and was washed successively with saturated aqueous copper(II) acetate, 10% HCl, saturated sodium bicarbonate, and brine. The organic layer was then dried with magnesium sulfate and the solvent removed *in vacuo* to yield a slightly brown solid. This crude product (2.2 g) was used directly without any further purification.

The crude mesylate (2.2 g, 4.8 mmol) was dissolved in 20 mL of DMF under argon. Sodium azide (760 mg, 11.7 mmol) was added and the reaction was stirred vigorously at room temperature overnight. The mixture was then poured into an ice−water mixture and the solid was filtered out and washed with water. Flash chromatography (7:3 ethyl acetate:hexanes) followed by recrystallization from ether and hexanes yielded 1.6 g (68.2% over three steps) of **16** as a pure white powder. Characterization data are consistent with that reported previously in the literature.[32] ^{1}H NMR (400 MHz, CDCl$_3$): δ_{ppm} 5.42 (dd, 1H, J = 3.1, 3.1 Hz), 5.25 (dd, 1H, J = 8.7, 4.7 Hz), 5.18 (dd, 1H, J = 8.7, 3.3 Hz), 4.34−4.32 (m, 2H), 4.09 (ddd, 2H, J = 7.8, 5.9, 3.4 Hz), 3.43−3.41 (m, 2H), 2.12 (s, 3H), 2.10 (s, 3H), 2.07 (s, 3H), 2.05 (s, 3H), 1.99−1.87 (m, 1H), 1.75−1.65 (m, 1H). ^{13}C NMR (100 MHz, CDCl$_3$): δ_{ppm} 170.6, 170.0, 169.8, 169.7, 69.0, 68.9, 68.2, 67.9, 67.2, 61.2, 47.7, 26.0, 20.8, 20.8, 20.7. ESI-MS m/z calcd for C$_{16}$H$_{23}$N$_3$O$_9$ [M+H]$^+$: 402.151; [M+Na]$^+$: 424.133. Found: 402.13, 424.11.

(2,3,4,6-Tetra-*O*-acetyl-α-D-galactopyranosyl)methyl Azide (24). Azido sugar **24** was synthesized according to a modified procedure[33] as indicated in Scheme 1 in the Supporting Information. Spectral data are consistent with previously published data. ^{1}H NMR (400 MHz, CDCl$_3$): δ_{ppm} 5.44 (dd, 1H, J = 3.3, 3.3 Hz), 5.27 (dd, 1H, J = 8.4, 4.6 Hz), 5.22 (dd, 1H, J = 8.4, 3.2 Hz), 4.39 (m, 2H), 4.25 (ddd, 1H, J = 8.0, 4.5, 3.4 Hz), 4.11 (dd, 1H, J = 11.7, 4.7 Hz), 3.63 (dd, 1H, J = 13.5, 8.8 Hz), 3.24 (dd, 1H, J = 13.5, 3.7 Hz), 2.12 (s, 3H), 2.11 (s, 3H), 2.07 (s, 3H), 2.06 (s, 3H). ^{13}C NMR (100 MHz, CDCl$_3$): δ_{ppm} 170.7, 169.8, 169.6, 169.5, 70.8, 69.8, 67.7, 67.5, 66.9, 60.7, 48.3, 20.67, 20.66, 20.59. ESI-MS m/z calcd for C$_{15}$H$_{21}$N$_3$O$_9$ [M + K]$^+$: 426.091. Found: 426.12.

(2*S*)-1-Allyl-2-[[(9*H*-Fluoren-9-ylmethoxy)carbonyl]amino]-3-(4-(2,3,4,6-tetra-*O*-acetyl-α-D-galactopyranosyl)-2,3,4-triazol-1-yl)-propanoate (15). Compounds **13** (10 mg, 0.027 mmol) and **14** (10 mg, 0.027 mmol) were dissolved in 200 μL of the organic solvent and 150 μL of water in a 3 mL culture tube. A 0.2 M cupric acetate solution (25 μL, 0.005 mmol) was then added and the reaction was sealed with a septum. The tube was flushed with argon for 10 min and then placed in a 40 °C oil bath. A 0.4 M sodium ascorbate solution (25 μL, 0.01 mmol) was added and the reaction was stirred until completion (for a maximum of 6 h). The reaction mixture was then cooled to room temperature, diluted with ethyl acetate, and washed with water and brine. Solvent was removed *in vacuo* and the crude product was purified by preparative TLC (6:4 ethyl acetate:hexanes). ^{1}H NMR (400 MHz, CDCl$_3$): δ_{ppm} 7.76 (d, 2H, J = 7.5 Hz), 7.61 (t, 2H, J = 7.3 Hz), 7.40 (ddd, 2H, J = 7.4, 7.4, 3.3 Hz), 7.37−7.29 (m, 3H), 6.38 (d, 1H, J = 6.1 Hz), 6.16 (dd,

1H, $J = 10.7, 3.3$ Hz), 5.97−5.86 (m, 1H), 5.85 (d, 1H, $J = 8.2$ Hz), 5.65 (d, 1H, $J = 3.1$ Hz), 5.46 (dd, 1H, $J = 10.8, 6.0$ Hz), 5.35 (d, 1H, $J = 17.1$ Hz), 5.27 (d, 1H, $J = 10.4$ Hz), 4.73 (ddd, 1H, $J = 8.2, 5.2, 5.2$ Hz), 4.64 (d, 2H, $J = 5.6$ Hz), 4.60 (dd, 1H, $J = 6.4, 6.4$ Hz), 4.39 (d, 2H, $J = 7.1$ Hz), 4.24 (dd, 1H, $J = 7.0, 7.0$ Hz), 4.10 (dd, 1H, $J = 11.3, 6.6$ Hz), 4.00 (dd, 1H, $J = 11.3, 6.5$ Hz), 3.32 (d, 2H, $J = 5.1$ Hz), 2.19 (s, 3H), 2.01 (s, 3H), 1.95 (s, 3H), 1.88 (s, 3H). ^{13}C NMR (100 MHz, CDCl$_3$): δ_{ppm} 170.6, 170.6, 170.3, 170.0, 169.4, 155.9, 143.8, 143.7, 142.0, 141.3, 141.2, 131.4, 127.8, 127.1, 127.1, 125.1, 124.5, 120.0, 119.2, 81.7, 70.5, 67.7, 67.5, 67.2, 67.2, 66.2, 61.2, 53.4, 47.1, 28.0, 20.61, 20.61, 20.6, 20.3. ESI-MS m/z calcd for C$_{37}$H$_{40}$N$_4$O$_{13}$ [M+H]$^+$: 749.2665; [M+Na]$^+$: 771.2490. Found: 749.22, 771.20.

(2S)-1-Allyl-2-[[(9H-fluoren-9-ylmethoxy)carbonyl]amino]-3-(4-(2,3,4,6-tetra-O-acetyl-α-D-galactopyranosylethyl)-2,3,4-triazol-1-yl)-propanoate (17). Compounds **13** (10 mg, 0.027 mmol) and **16** (11 mg, 0.027 mmol) were treated with the same conditions as the preparation of **15**. The crude product **17** was purified by preparative TLC (7:3 ethyl acetate: hexanes). ^{1}H NMR (400 MHz, CDCl$_3$): δ_{ppm} 7.76 (d, 2H, $J = 7.5$ Hz), 7.59 (t, 2H, $J = 7.4$ Hz), 7.40 (t, 2H, $J = 7.4$ Hz), 7.37 (s, 1H), 7.31 (t, 2H, $J = 7.5, 7.5$ Hz), 5.94 (d, 1H, $J = 8.9$ Hz), 5.89 (m, 1H), 5.41 (t, 1H, $J = 2.8, 2.8$ Hz), 5.32 (d, 1H, $J = 17.1$ Hz), 5.25 (dd, 1H, $J = 10.4, 1.1$ Hz), 5.20 (d, 1H, $J = 4.5$ Hz), 5.17 (dd, 1H, $J = 8.7, 3.1$ Hz), 4.73 (dd, 1H, $J = 13.3, 5.4$ Hz), 4.66 (d, 2H, $J = 5.7$ Hz), 4.46 (ddd, 1H, $J = 12.9, 7.9, 4.8$ Hz), 4.41−4.27 (m, 4H), 4.23 (dd, 1H, $J = 7.2, 7.2$ Hz), 4.19−4.13 (m, 1H), 4.11−4.02 (m, 2H), 3.31 (d, 2H, $J = 4.9$ Hz), 2.31−2.17 (m, 1H), 2.10 (s, 3H), 2.07 (s, 6H), 2.03 (s, 3H). ^{13}C NMR (100 MHz, CDCl$_3$): δ_{ppm} 170.8, 170.6, 169.9, 169.7, 169.7, 156.0, 143.8, 143.8, 142.7, 141.2, 141.2, 131.6, 127.7, 127.1, 125.2, 125.2, 122.8, 120.0, 118.7, 77.5, 77.2, 76.9, 69.2, 68.6, 68.0, 67.7, 67.1, 66.1, 61.1, 53.5, 47.1, 46.4, 28.1, 27.1, 20.77, 20.74, 20.71, 20.63. ESI-MS m/z calcd for C$_{39}$H$_{44}$N$_4$O$_{13}$ [M+H]$^+$: 777.2978. Found: 777.21.

General Method for Peptide Synthesis. The syntheses of the peptides were carried out using an Advanced Chem Tech Apex 396 automated peptide synthesizer (40 wells), equipped with a dual-arm system and argon atmosphere controlled from an IBM PC using *Advanced Chem Tech* v 1.6 software. Preloaded Fmoc-Gly-Wang or Fmoc-Ala-Wang resins were swollen in DMF for 1 h followed by filtration, and then were subjected to 20% piperidine in DMF twice successively for 30 min. Peptide couplings were performed using standard conditions for Fmoc solid-phase synthesis using HCTU as coupling agent.[34] Following the coupling of each residue, deprotection of the Fmoc moiety was accomplished by treatment with 20% piperidine in DMF. Between each deprotection and coupling, and after every coupling, the beads were shaken 4 times with 4 mL of DMF followed by filtration. Upon completion of the synthesis, the beads were washed extensively with DMF (6 × 4 mL), MeOH (6 × 4 mL), DCM (6 × 4 mL), hexanes (6 × 4 mL), and ethanol (3 × 6 mL) and then removed from the synthesizer and stored in a desiccator under vacuum in the presence of P$_2$O$_5$ until required. A small amount of the peptide was cleaved from the resin for characterization using 92.5:5:2.5 (v/v/v) TFA:triisopropylsilane:water. The peptides were purified using reversed-phase HPLC (ramp from 0% to 18% acetonitrile in water over 5 min followed by isocratic flow for 25 min) unless stated otherwise.

Resin-Supported Peptide 18. Peptide **18** was prepared using 100 mg of Wang resin using standard Fmoc-based SPS

protocols.[34] 5 mg of resin was directly cleaved and the crude peptide was purified through preparatory TLC (30% water in methanol) to yield 0.8 mg of **18** as a white powder (91% based on resin loading). ^{1}H NMR (400 MHz, D$_2$O): δ_{ppm} 3.94−3.78 (m, 5H), 3.59 (d, 2H, $J = 1.35$ Hz), 2.64 (d, 2H, $J = 3.23$ Hz, 2H), 2.36 (t, 1H, $J = 2.21$). ^{13}C NMR (100 MHz, D$_2$O): δ_{ppm} 171.4, 171.32, 171.31, 168.9, 76.2, 74.4, 51.4, 42.6, 42.4, 42.3, 21.0. ESI-MS m/z calcd for C$_{11}$H$_{16}$N$_4$O$_5$ [M+H]$^+$: 285.1199. Found: 285.072.

Resin-Supported Peptide 20. Peptide **20** was prepared using 115 mg of Wang resin using standard Fmoc-based SPS protocols.[34] 18 mg of resin was cleaved directly and purified by reversed-phase HPLC to yield 3.0 mg of **20** as a white powder in 78% yield (based on resin loading). ^{1}H NMR (400 MHz, D$_2$O): δ_{ppm} 7.40−7.15 (m, 5H), 4.60 (dd, 1H, $J = 8.2, 6.6$ Hz), 4.30 (q, 1H, $J = 7.3$ Hz), 4.19 (t, 1H, $J = 6.1$ Hz), 3.91 (q, 2H, $J = 16.9$ Hz), 3.11 (dd, 1H, $J = 13.9, 6.5$ Hz), 2.96 (dd, 1H, $J = 13.9, 8.3$ Hz), 2.84 (td, 2H, $J = 3.3, 2.9$ Hz), 2.52 (t, 1H, $J = 2.7$ Hz), 1.33 (d, 3H, $J = 7.3$ Hz). ^{13}C NMR (125 MHz, D$_2$O): δ_{ppm} 176.7, 173.2, 171.0, 169.3, 136.8, 129.9, 129.4, 127.8, 83.2, 75.1, 55.4, 52.0, 49.3, 42.869, 42.861, 37.9, 21.7. ESI-MS m/z calcd for C$_{19}$H$_{24}$N$_4$O$_5$ [M+H]$^+$: 389.182; [M+Na]$^+$: 411.164. Found: 389.19, 411.17.

Resin-Supported Peptide 23. Peptide **23** was prepared using 115 mg of Wang resin according to standard Fmoc-based SPS protocols.[34] 10 mg of resin was cleaved directly and purified by reversed-phase HPLC to yield 1.8 mg of **23** as a white powder in 70% yield (based on resin loading). ^{1}H NMR (400 MHz, D$_2$O): δ_{ppm} 4.58 (m, 3H), 4.29 (t, 1H, $J = 5.9$ Hz), 4.19−3.79 (m, 18H), 2.93 (dd, 2H, $J = 5.9, 2.8$ Hz), 2.76 (bd, 6H, $J = 6.1$ Hz), 2.60 (t, 1H, $J = 2.5$ Hz), 2.46 (t, 3H, $J = 2.4$ Hz). ^{13}C NMR (125 MHz, D$_2$O): δ_{ppm} 172.7, 171.8, 171.5, 171.3, 168.8, 79.2, 76.2, 74.3, 72.2, 52.4, 52.3, 51.3, 42.5, 42.4, 42.2, 20.8. ESI-MS m/z calcd for C$_{38}$H$_{49}$N$_{13}$O$_{14}$ [M+H]$^+$: 912.3595; [M+Na]$^+$: 934.3420. Found: 912.34, 934.32.

Resin-Supported Peptide 25. Peptide **25** was prepared using 150 mg of Wang resin using standard Fmoc-based SPS protocols with amino acid **26** (Scheme 3b).[34] 20 mg of resin was directly cleaved and the crude peptide was purified by reversed-phase HPLC (isocratic flow with 10% acetonitrile in water for 5 min followed by a linear gradient from 10% to 60% acetonitrile in water) to yield 4.1 mg of **25** as a white powder in 48% yield (based on resin loading). ^{1}H NMR (500 MHz, D$_2$O, presaturation on HOD): δ_{ppm} 4.36 (m, 3H), 3.90−3.75 (m, 17H), 3.60 (s, 2H), 2.28−2.09 (m, 12H), 1.91 (m, 4H), 1.80 (m, 4H). ^{13}C NMR (125 MHz, D$_2$O): δ_{ppm} 176.4, 174.2, 174.2, 174.1, 171.9, 171.8, 171.7, 171.6, 171.5, 170.9, 83.3, 82.6, 70.8, 70.3, 52.9, 52.8, 52.8, 52.6, 43.1, 42.5, 42.4, 42.3, 29.3, 29.2, 14.4, 13.9. ESI-MS m/z calcd for C$_{42}$H$_{58}$N$_{13}$O$_{14}$ [M+H]$^+$: 968.42. Found: 968.76.

(S)-2-(9-Fluorenylmethoxycarbonylamino)-hex-5-ynoic Acid (26). Amino acid **26** was synthesized as indicated in Scheme 2 in the Supporting Information. ^{1}H NMR (CDCl$_3$/CD$_3$OD 2/1, 400 MHz): δ_{ppm} 7.71 (d, 2H, $J = 7.6$ Hz), 7.58 (dd, 2H, $J = 7.1, 3.9$ Hz), 7.35 (t, 2H, $J = 7.6$ Hz), 7.27 (t, 2H, $J = 7.6$ Hz), 4.35 (m, 3H), 4.18 (t, 1H, $J = 6.8$ Hz), 2.24 (m, 2H), 2.09 (m, 1H), 2.01 (t, 1H, $J = 2.6$ Hz), 1.86 (m, 1H). ^{13}C NMR (CDCl$_3$/CD$_3$OD 2/1, 100 MHz): δ_{ppm} 173.9, 156.7, 143.8, 143.7, 141.2, 141.2, 127.7, 127.0, 125.0, 119.8, 82.6, 77.5, 69.3, 66.9, 53.0, 47.1, 30.9, 14.9. ESI-MS m/z calcd for C$_{21}$H$_{19}$NO$_4$ [M + Na]$^+$: 372.12. Found: 372.24.

General Protocol for the Solid-Phase Organic Synthesis Microwave "Click" Reaction. A CEM Mars X Microwave System with 300 W maximum power and quartz reaction vessels

was used for these reactions. The resin supported peptide was initially stirred in DMF for 30 min under argon. Five equivalents of azide per mole of alkyne and 0.2 equiv of cupric acetate per mol of alkyne were added and the solution was degassed under argon. 0.4 equivalents of sodium ascorbate per mole of alkyne was then added and the stirbar was removed. The flask was sealed under argon and placed in the microwave and run under the following conditions: 2 min ramp to 90 °C then held at 15% power for 1.5 h. The solvent was then drained, and the beads were washed extensively with 1:1 water:isopropanol followed by 4 × 4 mL DMF, 4 × 4 mL MeOH, 4 × 4 mL DCM, and finally 4 × 4 mL hexanes. The beads were then stirred in 4 mL of 92.5:5:2.5 TFA:triisopropylsilane:water cleavage cocktail to remove the product off the resin. Solvent was evaporated at ambient temperature. The residue was washed with ether (4 × 5 mL), then dissolved in a solution of 0.01 M sodium methoxide in methanol with a drop of water and stirred for 1.5 h at room temperature. TFA was added until the pH of the solution was adjusted to 6. The mixture was evaporated to dryness, desalted, and resuspended in water and purified by reversed-phase HPLC.

Glycopeptide 21. Resin-supported **20** (80 mg, 0.046 mmol) was treated as per the general procedure described above with **14** (85.2 mg, 0.23 mmol), cupric acetate (1.7 mg, 0.0093 mmol), and sodium ascorbate (3.4 mg, 0.017 mmol). Purification by reversed-phase HPLC (1% acetonitrile in water for 12 min followed by a linear gradient from 1% acetonitrile in water to 10% acetonitrile in water over 28 min followed by a linear gradient from 10% acetonitrile in water to 98% acetonitrile in water over 40 min) yielded 16.7 mg of **21** as a white powder (61% based on resin-loading). ^{1}H NMR (500 MHz, D$_2$O): δ_{ppm} 8.01 (s, 1H), 7.38−7.15 (m, 5H), 6.26 (s, 1H), 4.69−4.56 (m, 1H), 4.51−4.42 (m, 1H), 4.35−4.15 (m, 2H), 4.13−3.96 (m, 3H), 3.89−3.75 (m, 2H), 3.70−3.56 (m, 2H), 3.33−3.09 (m, 3H), 3.04−2.95 (m, 1H), 1.33−1.18 (m, 3H). ^{13}C NMR (125 MHz, D$_2$O): δ_{ppm} 179.4, 171.8, 170.860, 170.7, 136.6, 129.1, 128.6, 1267.0, 74.9, 69.2, 68.7, 66.8, 61.1, 54.8, 54.2, 46.5, 42.4, 36.7, 17.5. ESI-MS m/z calcd for C$_{25}$H$_{35}$N$_7$O$_{10}$ [M + H]$^+$: 594.25. Found: 594.42.

Glycopeptide 22. Resin-supported **20** (24 mg, 0.0137 mmol) was treated as per the general procedure described above with **16** (27.5 mg, 0.0685 mmol), cupric acetate (0.5 mg, 0.0028 mmol), and sodium ascorbate (1 mg, 0.0051 mmol). Purification by reversed-phase HPLC (2% acetonitrile in water for 9 min followed by a linear gradient from 2% acetonitrile in water to 40% acetonitrile in water over 30 min) yielded 6 mg of **22** as a white powder (70% based on resin-loading). ^{1}H NMR (500 MHz, D$_2$O): δ_{ppm} 7.76 (s, 1H), 7.27−7.09 (m, 5H), 4.37 (dd, 2H, J = 14.0, 6.3 Hz), 4.18 (t, 1H, J = 6.3 Hz), 4.02 (dd, 1H, J = 14.3, 7.0 Hz), 3.76−3.85 (m, 3H), 3.74 (d, 1H, J = 1.6 Hz), 3.66−3.58 (m, 2H), 3.55 (d, 2H, J = 5.8 Hz), 3.18 (d, 1H, J = 6.3), 3.07 (dd, 1H, J = 13.9, 5.4 Hz), 2.87 (dd, 1H, J = 13.9, 9.3 Hz), 2.30−1.99 (m, 2H), 1.19 (d, 3H, J = 7.2 Hz). ^{13}C NMR (125 MHz, D$_2$O): δ_{ppm} 171.9, 170.4, 169.0, 162.8, 136.4, 129.2, 128.6, 127.0, 72.1, 69.5, 68.7, 67.6, 60.9, 54.8, 52.6, 47.0, 42.2, 36.9, 26.6, 24.6, 17.2. ESI-MS m/z calcd for C$_{27}$H$_{39}$N$_7$O$_{10}$ [M+H]$^+$: 622.284; [M+Na]$^+$: 644.266. Found: 622.15, 644.18.

Glycopeptide 9. Resin-supported **23** (60 mg 0.026 mmol) was treated as per the general procedure described above with **14** (190 mg, 0.51 mmol), cupric acetate (3.8 mg, 0.020 mmol), and sodium ascorbate (8.2 mg, 0.041 mmol). Purification by

reversed-phase HPLC (1% acetonitrile in water for 12 min followed by a linear gradient from 1% acetonitrile in water to 10% acetonitrile in water over 28 min followed by a linear gradient from 10% acetonitrile in water to 98% acetonitrile in water over 40 min) yielded 9 mg of **9** as a white powder (20% based on resin loading). ^{1}H NMR (500 MHz, D$_2$O): δ_{ppm} 7.83 (s, 4H), 6.12 (d, 4H, J = 5.9 Hz), 4.33 (d, 4H, J = 10.1 Hz), 4.17 (dd, 4H, J = 10.0, 6.3 Hz), 3.93 (m, 5H), 3.86−3.71 (m, 17H), 3.60−3.47 (m, 12H), 3.18−2.98 (m, 12H). ^{13}C NMR (125 MHz, D$_2$O): δ_{ppm} 173.2, 173.0, 172.0, 171.9, 171.83, 171.76, 171.3, 171.28, 171.22, 171.1, 148.8, 125.3, 85.2, 74.8, 69.3, 68.7, 67.0, 61.1, 53.2, 53.16, 53.14, 46.57, 42.59, 42.2, 27.1, 26.9, 26.8, 26.7, 26.65, 26.59, 25.1, 23.7. MALDI-TOF MS m/z calcd for C$_{62}$H$_{93}$N$_{25}$O$_{34}$ [M + Na + H]$^{2+}$: 877.814. Found: 877.8.

Glycopeptide 10. Resin-supported **23** (70 mg 0.030 mmol) was treated as per the general procedure described above with **24** (94 mg, 0.24 mmol), cupric acetate (6.5 mg, 0.036 mmol), and sodium ascorbate (13 mg, 0.072 mmol). Purification by reversed-phase HPLC (1% acetonitrile in water for 12 min followed by a linear gradient from 1% acetonitrile in water to 10% acetonitrile in water over 28 min followed by a linear gradient from 10% acetonitrile in water to 98% acetonitrile in water over 40 min) yielded 25 mg of **10** as a white powder (45% based on resin loading). ^{1}H NMR (500 MHz, D$_2$O): δ_{ppm} 7.73 (s, 4H), 4.53 (m, 4H), 4.24 (s, 4H), 3.93 (m, 5H), 3.88−3.63 (m, 28H), 3.59−3.56 (m, 5H), 3.54−3.38 (m, 12H), 3.13−2.97 (m, 8H). ^{13}C NMR (125 MHz, D$_2$O): δ_{ppm} 171.4, 171.3, 171.2, 171.1, 171.1, 171.0, 170.9, 129.8, 122.6, 74.7, 74.6, 74.5, 72.5, 69.5, 69.4, 69.2, 68.7, 68.6, 68.4, 67.1, 60.8, 45.74, 45.70, 45.6, 42.6, 42.4, 42.3, 42.2, 27.2, 27.13, 27.09, 27.02. MALDI-TOF MS m/z calcd for C$_{66}$H$_{101}$N$_{25}$O$_{34}$ [M + H]$^+$: 1788.69. Found: 1788.6.

Glycopeptide 11. Resin-supported **23** (40 mg 0.017 mmol) was treated as per the general procedure described above with **16** (136 mg, 0.34 mmol), cupric acetate (2.5 mg, 0.0136 mmol), and sodium ascorbate (5.5 mg, 0.0275 mmol). Purification by reversed-phase HPLC (2% acetonitrile in water for 9 min followed by a linear gradient from 2% acetonitrile in water to 40% acetonitrile in water over 30 min) yielded 17 mg of **11** as a white powder (54% based on resin loading). ^{1}H NMR (500 MHz, D$_2$O): δ_{ppm} 7.84 (s, 1H), 7.76 (s, 3H), 4.62−4.51 (m, 4H), 4.40−4.32 (m, 9H), 4.26 (t, 1H, J = 6.40 Hz), 3.92−3.70 (m, 24H), 3.63 (dd, 12H, J = 10.1, 3.0 Hz), 3.58−3.53 (m, 8H), 3.25 (d, 2H, J = 6.2 Hz), 3.21−2.96 (m, 6H), 2.24−2.10 (m, 4H), 1.95−2.10 (m, 4H). ^{13}C NMR (125 MHz, D$_2$O): δ_{ppm} 173.0, 172.0, 171.87, 171.80, 171.69, 171.42, 171.4, 171.36, 171.32, 171.19, 169.8, 169.3, 126.2, 126.1, 72.2, 72.1, 72.0, 69.6, 68.8, 67.7, 65.8, 61.0, 54.4, 53.8, 53.3, 52.7, 47.0, 46.95, 46.91, 42.6, 42.6, 42.3, 42.2, 27.9, 27.2, 27.0, 26.9, 26.8, 26.6, 24.6, 22.2. MALDI-TOF MS m/z calcd for C$_{70}$H$_{109}$N$_{25}$O$_{34}$ [M]$^+$: 1843.76. Found: 1843.8.

Glycopeptide 12. Resin-supported **25** (25 mg, 0.011 mmol) was treated as per the general procedure described above with **24** (85 mg, 0.22 mmol), cupric acetate (1.6 mg, 0.009 mmol), and sodium ascorbate (3.6 mg, 0.018 mmol). Purification by reversed-phase HPLC (isocratic 1% acetonitrile in water for 10 min followed by a linear gradient from 1% acetonitrile in water to 30% acetonitrile in water over 30 min) yielded 3.3 mg of **12** as a white powder (16% based on resin loading). ^{1}H NMR (500 MHz, D$_2$O, presaturation on HOD): δ_{ppm} 7.71 (br s, 4H), 4.31 (s, 4H), 4.17 (s, 3H), 4.08−3.43 (m, 51H), 2.65 (m, 8H), 2.05−1.77 (m, 8H). ^{13}C NMR (125 MHz, D$_2$O): δ_{ppm} 174.2, 171.8, 171.0, 124.0, 96.4, 74.8, 72.5, 69.6, 68.7, 67.1, 60.8, 52.8, 45.5, 43.1, 42.5,

Table 1. Optimization of Solution-Phase "Click" Coupling
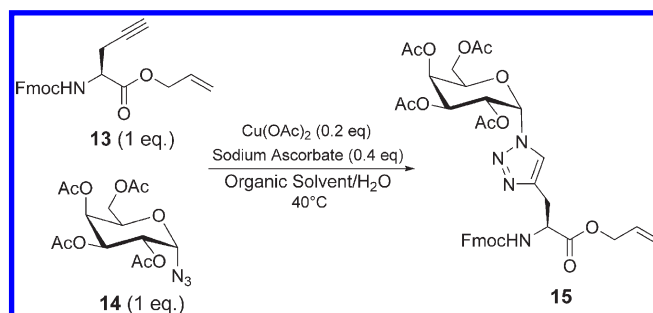
	organic solvent	solvent composition (% organic)	reaction time (hrs)	% conversion[a]
1	t-BuOH	50	5	81
2	DMF	50	4	76
3	NMP	50	3	>98
4	Dioxane	50	1	95
5	THF	50	0.5	>98
6	THF	75	0.75	>98
7	THF	80	0.25	>98
8	THF	90	0.5	>98
9[b]	THF	90	0.25	>98

[a] Conversions calculated based upon analysis of crude reaction mixture using ^{1}H NMR. [b] Reaction carried out with **5** equiv of azide.

Table 2. Optimization of Solvent Conditions Using a Primary Azido Sugar
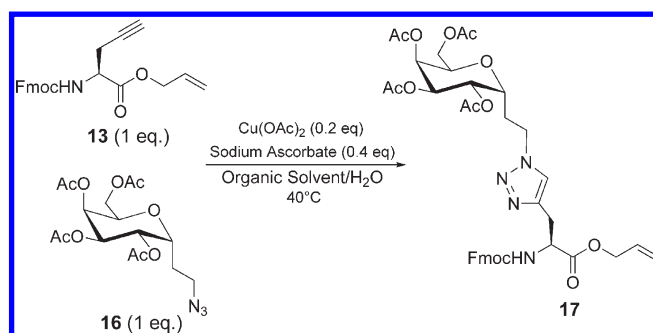
	organic solvent	solvent composition (% organic)	reaction time (hrs)	conversion[a]
1	DMF	50	0.25	78
2	NMP	50	0.5	>98
3	Dioxane	50	0.5	>98
4	THF	50	0.5	>98

[a] Conversions calculated based upon analysis of crude reaction mixture using ^{1}H NMR.

42.3, 30.1, 20.9. MALDI-TOF MS m/z calcd for $C_{70}H_{109}N_{25}O_{34}$ $[M + Na]^+$: 1866.7. Found: 1867.5.

■ RESULTS AND DISCUSSION

Several modifications to the original "Click" reaction conditions for solid-phase applications have been reported.[16,17,35−39] We sought to utilize solvents that would permit reaction conditions with sub-stoichiometric amounts of copper and also facilitate swelling of the solid-phase resin. As a result, a number of organic solvents capable of swelling Wang resin were examined for the solution-phase reaction between alkyne **13** and azido sugar **14** before applying the conditions to the solid-phase synthesis of triazole-containing C-AFGP analogues.[40] The reaction between **13** and **14** was investigated using aqueous mixtures (50%) of N-methyl morpholine (NMP), tetrahydrofuran (THF), N,N-dimethyl formamide (DMF), dioxane and tert-butanol (Table 1). All of these solvents have excellent swelling properties for Wang resin except for tert-butanol, which swells resins poorly.[40] Under typical Sharpless reaction conditions

Scheme 1. Solid-Phase Synthesis of a Triazole-Linked Glycopeptide Using Optimized Conditions
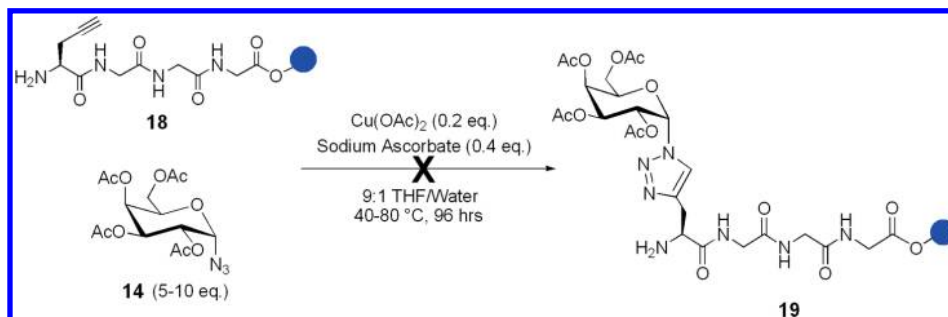
Scheme 2. Microwave Assisted Solid-Phase Synthesis of Triazole-Linked Glycopeptides
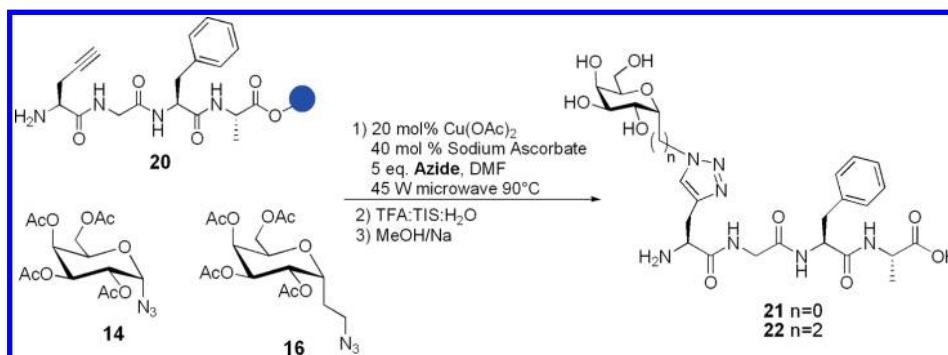
using *tert*-butanol,[11] **15** was formed, but reaction conversion was only 81% after 5 h (Table 1, entry 1). DMF resulted in only 76% conversion after 4 h (entry 2), while NMP resulted in complete conversion after 3 h (entry 3). In contrast, dioxane afforded 95% conversion after only 1 h (entry 4). However, the best results were obtained when THF was employed, with complete conversion after only 30 min (entry 5).

These solvent mixtures were also applicable with other azide substrates (Table 2). For instance, reaction of alkyne **13** with azido sugar **16** yielded similar results to those described above, but reaction times were generally shorter. When DMF was used as a cosolvent, glycoconjugate **17** was obtained in 78% conversion after only 15 min (Table 2, entry 1), as opposed to 76% conversion in 4 h for glycoconjugate **15** prepared from azido sugar **14** (Table 1, entry 2). Quantitative conversions for **17** were also obtained within 30 min when NMP, dioxane, and THF were employed (Table 2, entries 2–4). Overall, THF yielded the best results, showing it to be an ideal solvent for the solution-phase coupling regardless of the structure of the azide substrate.

As stated previously, a solvent system with minimal water content is desirable for solid-phase applications to ensure an efficient swelling of the resin. However, an aqueous component is necessary to dissolve the sodium ascorbate and facilitate reduction of Cu(II) to Cu(I).[9,41] Hence, the efficiency of the solution-phase Click reaction of alkyne **13** with azido sugar **14** was repeated using a decreased percentage of water in THF (Table 1, entries 6–9). Surprisingly, decreasing the water content had no effect upon conversions and reaction times were still less than one hour (entries 6–8). However, the reaction time could further be reduced to 15 min without decreasing reaction

conversion by using a 10% water/THF solvent system in the presence of 5 equiv of azide (entry 9).

With optimized solution-phase results in hand, the solid-phase synthesis of a triazole-linked glycopeptide was attempted (Scheme 1). Initial attempts to couple resin-supported peptide **18** using the optimized conditions (10% water in THF, 0.2 equiv of Cu(OAc)$_2$, 0.4 equiv of sodium ascorbate) with azido sugar **14** (5 equiv) failed. Even upon heating the reaction for 96 h at 80 °C or adding 10 equiv of azido sugar **14**, the reaction still failed to yield glycopeptide **19**. Given the precedent for microwave accelerated Click couplings on solid-phase resins,[42] we investigated whether glycopeptide formation would occur in the presence of microwaves. Similar conditions were then attempted for the microwave accelerated "Click" coupling, but peptide **20** (Scheme 2) was utilized instead of **18**. Peptide **20** bearing a phenylalanine residue was selected, as the strong UV absorbance of this residue would facilitate purification by HPLC and anhydrous THF was used as the solvent. Consequently, resin-supported peptide **20** was reacted with azido sugar **14** in anhydrous THF, utilizing 0.2 equiv of Cu(OAc)$_2$, 0.4 equiv of sodium ascorbate, and microwave heating (300 W) for 2 h. Analysis by MALDI mass spectrometry of the crude reaction mixture failed to show a trace of product. However, when the solvent was changed to anhydrous DMF trace quantities of glycoconjugate **21** were detected after 2 h (the product was cleaved from the resin prior to analysis). By decreasing the power to 45 W, the reaction went to completion after only 1.5 h and glycoconjugate **21** was obtained in 61% yield after cleavage from the resin and subsequent deprotection and purification by reversed-phase HPLC (Scheme 2). Similarly, when resin-supported peptide **20** was reacted with azido sugar **16** under these

Scheme 3. Microwave Assisted Solid-Phase Synthesis of Glycopeptides 9−12
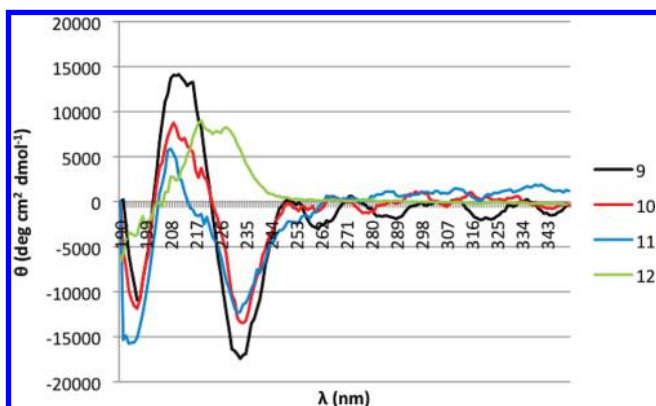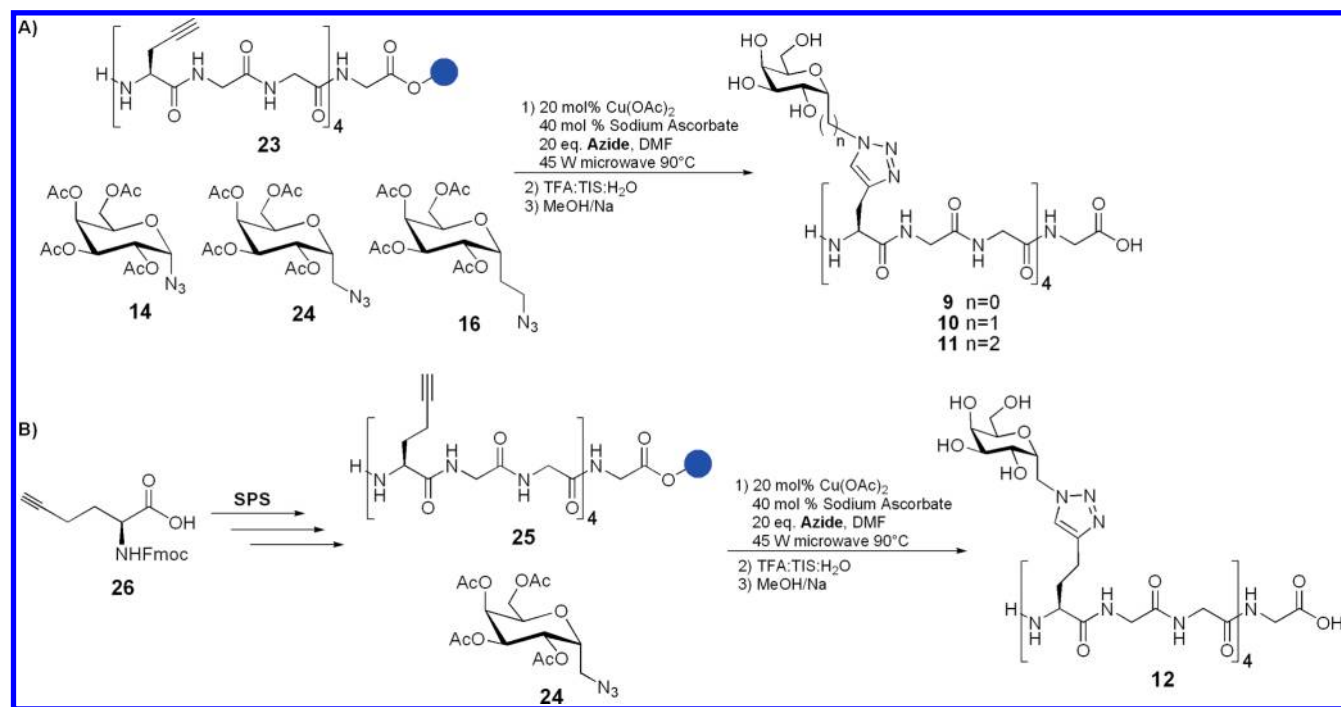
Figure 5. CD spectrum of glycopeptides 9−12. All spectra were acquired at 22 °C, with a concentration of 43 μM. CD data has been normalized for concentration and number of chromophores.

Table 3. Analysis of Secondary Structure for Glycopeptides 9−12

	α helix	β sheet	β turn	poly proline type 2	random coil
9	0.011	0.2975	0.1435	0.1225	0.4275
10	0.022	0.2505	0.1445	0.1125	0.469
11	0.0135	0.2855	0.1345	0.107	0.4555
12	0	0.358	0.093	0.193	0.356

reaction conditions, glycopeptide 22 was obtained in 70% isolated yield after cleavage from the resin, deprotection, and purification by reversed-phase HPLC.

With this promising result, the convergent syntheses of triazole-containing *C*-AFGP glycopeptides 9, 10, 11, and 12 were attempted. Glycosyl azide 14 and resin-supported peptide 23 (prepared under standard Fmoc solid-phase coupling conditions) were subjected to microwave heating in DMF with 0.2 equiv of Cu(OAc)$_2$ and 0.4 equiv of sodium ascorbate (Scheme 3a). Glycoconjugate 9 was obtained in 20% isolated yield following cleavage from the Wang resin, deprotection, and purification by reversed-phase HPLC. Similarly, reaction of azido sugar 24 with resin-supported peptide 23 yielded glycopeptide 10 (45% yield), and when azido sugar 16 was utilized, glycopeptide 11 was obtained in 54% yield. Glycosyl azide 24 was also

reacted with resin-supported peptide 25 (prepared under standard Fmoc solid-phase coupling conditions utilizing amino acid 26) under the microwave "Click" conditions described above, and glycopeptide 12 was obtained in 16% yield (Scheme 3b).

Triazole-containing AFGP analogues 9−12 were first examined for TH activity using a nanoliter osmometer.[28] This instrument is regarded as the "gold standard" for assessing thermal hysteresis. All four *C*-AFGP analogues were found to exhibit no thermal hysteresis activity. Furthermore, no dynamic ice shaping was evident indicating there was no interaction with the ice surface, a result consistent with the lack of thermal hysteresis activity in previously reported ornithine analogues 1−4.[4,6] Analysis of solution conformation using circular dichroism (CD) spectroscopy (Figure 5 and Table 3) suggests that the predominant secondary structure in solution is random coil with β-sheet being the next likely solution structure for glycopeptides 9−12. This is consistent with the solution conformation reported for AFGP-8 and other *C*-AFGP analogues studied by our laboratory[2,4,43] and suggests that the lack of TH activity is not due to the fact that AFGP analogues 9−12 adopt different solution conformations compared to the native AFGP.

The triazole-containing *C*-AFGP analogues 9−12 were also screened for their ability to inhibit ice recrystallization (IRI

Chart 1. IRI Activity of C-Linked AFGP Analogues[a]
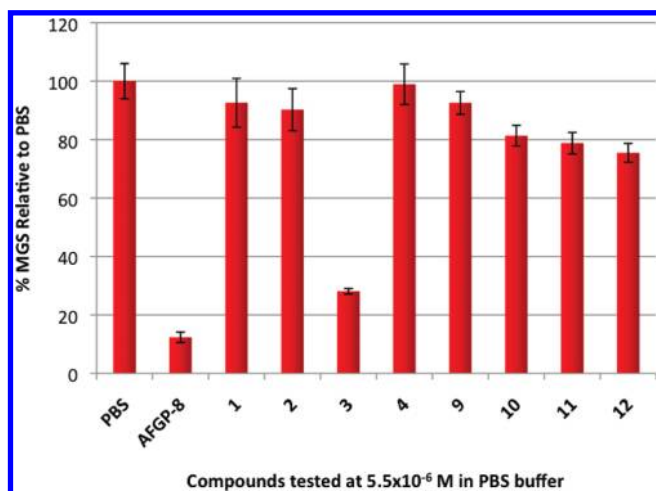
[a] PBS represents a positive control for ice recrystallization.

activity) using a splat cooling assay.[1,29] Chart 1 shows the IRI activity of triazole-containing C-AFGP analogues **9**−**12**, native AFGP-8, and previously synthesized C-AFGP analogues **1**−**4** (the latter contain an amide bond in the side chain).[6,44] In this assay, a phosphate buffered saline (PBS) solution is utilized as a positive control for ice recrystallization; thus, bars smaller than PBS indicate the ability to inhibit ice recrystallization. All samples have been normalized to PBS. As evident from Chart 1, triazole-containing AFGP analogue **9** failed to exhibit IRI activity. AFGP analogue **9** is closely related to peptoid AFGP analogue **6** (published by Norgren et al.) which also failed to exhibit IRI activity.[26] AFGP analogue **6** contains N-methyl glycine instead of glycine in the polypeptide backbone; however, the nature of the anomeric linkage, total length of the side chain, and the position of the triazole within the side chain are identical to those of AFGP analogue **9**. While these analogues did not inhibit the recrystallization of ice, the results are consistent with the suggestion that IRI activity is sensitive to the length of the side chain bearing the carbohydrate moiety. Similar results have been reported by our laboratory in analogues that contain an amide bond in the side
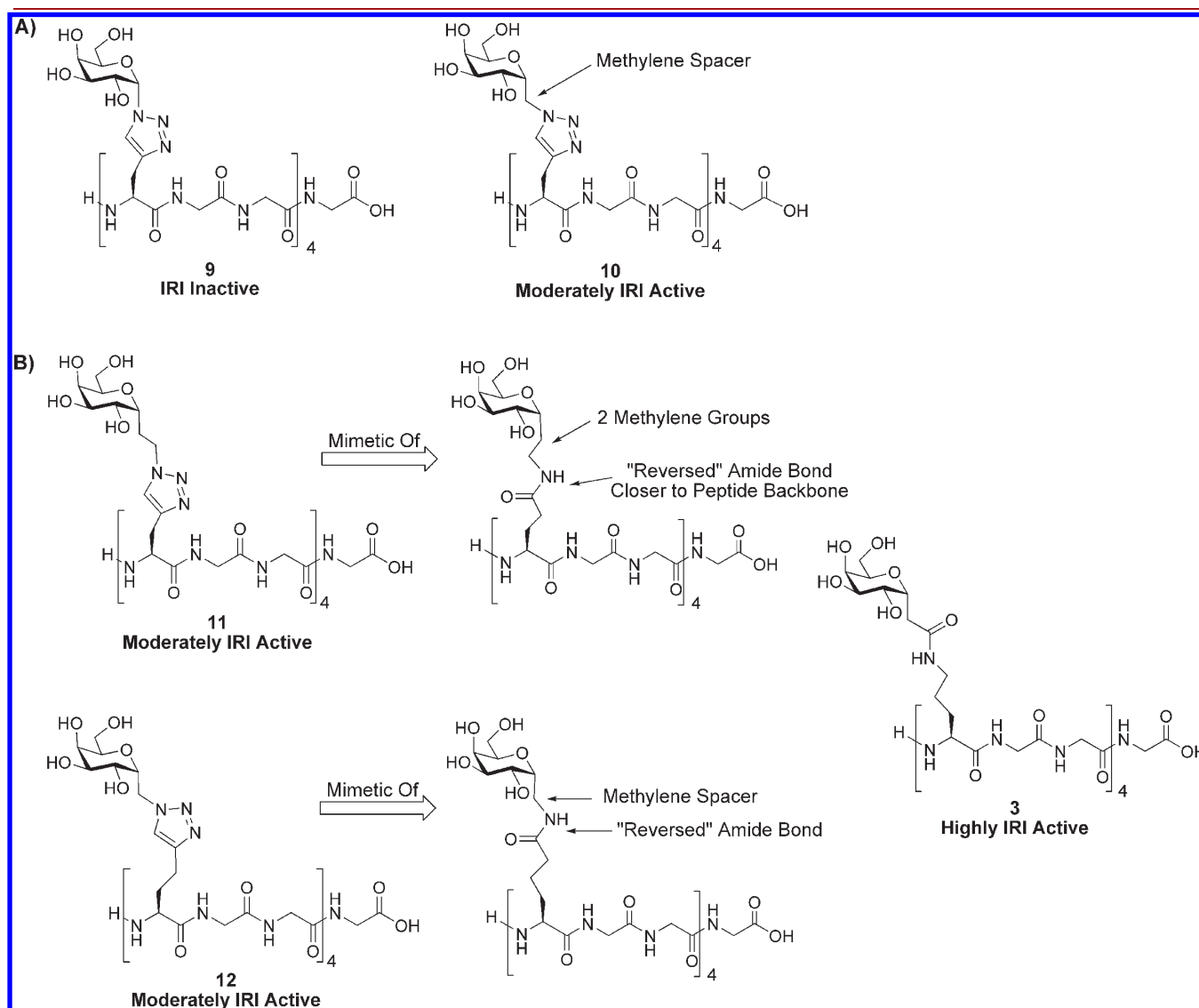
Figure 6. The presence of a hydrophobic methylene spacer and "reversed" directionality of the triazole moiety in AFGP analogues **9**−**12**.

chain instead of a triazole.[6] For instance, as the side chain of IRI active *C*-AFGP analogue **3** is shortened (compounds **1** and **2**) or lengthened (compound **4**) IRI activity is lost.[6]

Triazole-containing AFGP analogue **9** is also a close analogue of *C*-AFGP analogue **1**, which did not possess IRI activity. There are two key structural changes in AFGP analogue **9** relative to **1**. First, the triazole moiety has been employed to mimic the amide bond in **1**. Second, the orientation of the triazole in the side chain mimics an amide bond that is "reversed" in its orientation compared to **1**. These structural modifications in **9** do not restore IRI activity since this analogue failed to inhibit ice recrystallization. However, the fact that the lengths of the side chains in **9** and **1** are the same supports the hypothesis that the distance between the carbohydrate moiety and the peptide backbone is important for IRI activity.

Some of the most IRI active *C*-AFGP analogues prepared by our laboratory possess a methylene group between the carbohydrate moiety and the amide bond in the side chain. It has been proposed that the hydrophobic nature of this group is an important structural feature in *C*-AFGP analogue **3**. This methylene group is absent in triazole-containing AFGP analogue **9**. Interestingly, when this group is present as in triazole-containing *C*-AFGP analogue **10** (Figure 6a), the glycoconjugate is a moderate inhibitor of ice recrystallization, validating its importance.[6] Triazole-containing *C*-AFGP analogue **11** has two methylene groups incorporated between the carbohydrate moiety and the triazole linkage. This glycoconjugate has similar IRI activity as triazole-containing analogue **10**, further validating the importance of a hydrophobic group in the spacer close to the carbohydrate.[6] *C*-AFGP derivative **11** is also a close analogue of potent ice recrystallization inhibitor *C*-AFGP analogue **3**. However, **11** is not as active as **3**. The number of atoms between the carbohydrate moiety and the polypeptide backbone in analogues **3** and **11** is the same. However, the triazole moiety in **11** mimics an amide bond that has the directionality "reversed" relative to **3**. Furthermore, the position of the triazole linker in the side chain of **11** is different than the position of the amide bond in **3** (Figure 6b). The triazole linker in *C*-linked AFGP **11** is actually one atom closer to the polypeptide backbone than the amide bond in **3**. This structural modification is detrimental to IRI activity as analogue **11** is much less active than analogue **3**.

Triazole-containing *C*-AFGP analogue **12** is also a close analogue of **3** with the exception of the orientation of the triazole moiety. The orientation of the triazole mimics an amide bond that is "reversed" relative to **3** (Figure 6b). However, the length of the side chain between the carbohydrate and the peptide backbone, as well as the position of the triazole linker within this side chain, is the same (shown in Figure 6b). While triazole-containing analogue **12** exhibited moderate IRI activity, it is much less active than *C*-AFGP analogue **3**. These results indicate that while the presence of a hydrophobic methylene spacer and the length of the side chain bearing the triazole (or amide) linkage directly affect IRI activity, the amide bond in **3** is an essential structural feature necessary for potent IRI activity.

■ CONCLUSIONS

In summary, the synthesis of a series of triazole-containing AFGP and *C*-AFGP analogues has been reported. These compounds were prepared using a convergent solid-phase synthesis approach. "Click" chemistry conditions using Cu (II) (20 mol %) and sodium ascorbate as the *in situ* reductant in dry DMF in the presence of microwaves were utilized. Triazole-containing AFGP analogue **9** failed to exhibit IRI activity, while analogues **10**, **11**, and **12** exhibited moderate IRI activity. The results of this study suggest that substitution of the amide bond in *C*-AFGP analogue **3** with a triazole moiety is detrimental to IRI activity. In addition, a hydrophobic component (i.e., methylene spacer) close to the carbohydrate residue as well as the length of the side chain bearing the triazole (or amide) linkage is also important. This result is consistent with earlier findings by our laboratory. Molecular dynamics simulations and variable temperature NMR studies are currently being performed on analogues **10**, **11**, and **12** in an effort to elucidate how the methylene spacer and position of the triazole linker are influencing orientation of the carbohydrate residue. The results of these studies will be reported in due course.

■ ASSOCIATED CONTENT

ⓢ Supporting Information. Synthetic procedures for azido sugar **24**, amino acid **26**, and ^{1}H and ^{13}C spectra are available for all characterized compounds. This material is available free of charge via the Internet at http://pubs.acs.org.

■ AUTHOR INFORMATION

Corresponding Author
*rben@uottawa.ca.

■ ACKNOWLEDGMENT

■ REFERENCES

(1) Knight, C. A., Hallett, J., and DeVries, A. L. (1988) Solute effects on ice recrystallization: An assessment technique. *Cryobiology 25*, 55–60.

(2) DeVries, A. L., Komatsu, S. K., and Feeney, R. E. (1970) Chemical and physical properties of freezing point-depressing glycoproteins from Antarctic fishes. *J. Biol. Chem. 245*, 2901–2908.

(3) Bouvet, V., and Ben, R. N. (2003) Antifreeze glycoproteins: structure, conformation, and biological applications. *Cell Biochem. Biophys. 39*, 133–144.

(4) Czechura, P., Tam, R. Y., Dimitrijevic, E., Murphy, A. V., and Ben, R. N. (2008) The importance of hydration for inhibiting ice recrystallization with *C*-linked antifreeze glycoproteins. *J. Am. Chem. Soc. 130*, 2928–2929.

(5) Liu, S., and Ben, R. N. (2005) *C*-linked galactosyl serine AFGP analogues as potent recrystallization inhibitors. *Org. Lett. 7*, 2385–2388.

(6) Tam, R. Y., Rowley, C. N., Petrov, I., Zhang, T., Afagh, N. A., Woo, T. K., and Ben, R. N. (2009) Solution conformation of *C*-linked antifreeze glycoprotein analogues and modulation of ice recrystallization. *J. Am. Chem. Soc. 131*, 15745–15753.

(7) Tron, G. C., Pirali, T., Billington, R. A., Canonico, P. L., Sorba, G., and Genazzani, A. A. (2008) Click chemistry reactions in medicinal chemistry: applications of the 1,3-dipolar cycloaddition between azides and alkynes. *Med. Res. Rev. 28*, 278–308.

(8) Brik, A., Alexandratos, J., Lin, Y. C., Elder, J. H., Olson, A. J., Wlodawer, A., Goodsell, D. S., and Wong, C. H. (2005) 1,2,3-Triazole as a peptide surrogate in the rapid synthesis of HIV-1 protease inhibitors. *ChemBioChem 6*, 1167–1169.

(9) Rostovtsev, V. V., Green, L. G., Fokin, V. V., and Sharpless, K. B. (2002) A stepwise Huisgen cycloaddition process: copper(I)-catalyzed regioselective ligation of azides and terminal alkynes. *Angew. Chem., Int. Ed. 41*, 2596–2599.

(10) Tornøe, C. W., Christensen, C., and Meldal, M. (2002) Peptidotriazoles on solid phase: [1,2,3]-triazoles by regiospecific copper(I)-catalyzed 1,3-dipolar cycloadditions of terminal alkynes to azides. *J. Org. Chem. 67*, 3057–3064.

(11) Kolb, H. C., Finn, M. G., and Sharpless, K. B. (2001) Click chemistry: diverse chemical function from a few good reactions. *Angew. Chem. Intl. Ed. 40*, 2004–2021.

(12) van Dijk, M., Rijkers, D. T. S., Liskamp, R. M. J., van Nostrum, C. F., and Hennink, W. E. (2009) Synthesis and applications of biomedical and biodegradable polymers via Click chemistry methodologies. *Bioconjugate Chem. 20*, 2001–2016.

(13) Amblard, F., Cho, J. H., and Schinazi, R. F. (2009) Cu(I)-catalyzed Huisgen azide-alkyne 1,3-dipolar cycloaddition reaction in nucleoside, nucleotide, and oligonucleotide chemistry. *Chem. Rev. 109*, 4207–4220.

(14) Karskela, M., Helkearo, M., Virta, P., and Lönnberg, H. (2010) Synthesis of oligonucleotide glycoconjugates using sequential Click and oximation ligations. *Bioconjugate Chem. 21*, 748–755.

(15) Bera, S., Zhanel, G. G., and Schweizer, F. (2010) Evaluation of amphiphilic aminoglycoside-peptide triazole conjugates as antibacterial agents. *Bioorg. Med. Chem. Lett. 20*, 3031–3035.

(16) Pourceau, G., Meyer, A., Vasseur, J.-J., and Morvan, F. (2009) Synthesis of mannose and galactose oligonucleotide conjugates by bi-click chemistry. *J. Org. Chem. 74*, 1218–1222.

(17) Jølck, R. I., Berg, R. H., and Andresen, T. L. (2010) Solid-phase synthesis of PEGylated lipopeptides using click chemistry. *Bioconjugate Chem. 21*, 807–810.

(18) Meldal, M., Tornøe, C. W., Nielsen, T. E., Diness, F., Le Quement, S. T., Christensen, C. A., Feldthusen Jensen, J., Worm-Leonhard, K., Groth, T., Bouakaz, L., Wu, B., Hagel, G., and Keinicke, L. (2010) Ralph F. Hirschmann award address 2009: Merger of organic chemistry with peptide diversity. *Pept. Sci. 94*, 161–182.

(19) Oh, S., Jang, H. J., Ko, S. K., Ko, Y., and Park, S. B. (2010) Construction of a polyheterocyclic benzopyran library with diverse core skeletons through diversity-oriented synthesis pathway. *J. Comb. Chem. 12*, 548–558.

(20) Tachibana, Y., Matsubara, N., Nakajima, F., Tsuda, T., Tsuda, S., Monde, K., and Nishimura, S.-I. (2002) Efficient and versatile synthesis of mucin-like glycoprotein mimics. *Tetrahedron 58*, 10213–10224.

(21) Tachibana, Y., Fletcher, G. L., Fujitani, N., Tsuda, S., Monde, K., and Nishimura, S.-I. (2004) Antifreeze glycoproteins: elucidation of the structural motifs that are essential for antifreeze activity. *Angew. Chem., Int. Ed. 43*, 856–862.

(22) Ozawa, C., Hojo, H., Nakahara, Y., Katayama, H., Nabeshima, K., Akahane, T., and Nakahara, Y. (2007) Synthesis of glycopeptide dendrimer by a convergent method. *Tetrahedron 63*, 9685–9690.

(23) Conroy, T., Jolliffe, K. A., and Payne, R. J. (2009) Efficient use of the Dmab protecting group: applications for the solid-phase synthesis of N-linked glycopeptides. *Org. Biomol. Chem. 7*, 2255–2258.

(24) Kutterer, K. M. K., Barnes, M. L., and Arya, P. (1999) Automated, solid-phase synthesis of C-neoglycopeptides: coupling of glycosyl derivatives to resin-bound peptides. *J. Comb. Chem. 1*, 28–31.

(25) Miller, N., Williams, G. M., and Brimble, M. A. (2009) Synthesis of fish antifreeze neoglycopeptides using microwave-assisted "Click" chemistry. *Org. Lett. 11*, 2409–2412.

(26) Norgren, A. S., Budke, C., Majer, Z., Heggemann, C., Koop, T., and Sewald, N. (2009) On-resin Click-glycoconjugation of peptoids. *Synthesis* 488–494.

(27) Pedersen, D. S., and Rosenbohm, C. (2001) Dry vacuum column chromatography. *Synthesis* 2431–2434.

(28) Chakrabartty, A., and Hew, C. L. (1991) The effect of enhanced α-helicity on the activity of a winter flounder antifreeze polypeptide. *Eur. J. Biochem. 202*, 1057–1063.

(29) Jackman, J., Noestheden, M., Moffat, D., Pezacki, J. P., Findlay, S., and Ben, R. N. (2007) Assessing antifreeze activity of AFGP 8 using domain recognition software. *Biochem. Biophys. Res. Commun. 354* 340–344.

(30) Ibatullin, F. M., and Selivanov, S. I. (2002) Reaction of 1,2-trans-glycosyl acetates with phosphorus pentachloride: new efficient approach to 1,2-trans-glycosyl chlorides. *Tetrahedron Lett. 43*, 9577–9580.

(31) Szilágyi, L., and Györgydeák, Z. A. (1985) ^{13}C-N.M.R investigation of glycosyl azides and other azido sugars: stereochemical influences on the one-bond ^{13}C-^{1}H coupling constants. *Carbohydr. Res. 143*, 21.

(32) Podlipnik, C., Velter, I., La Ferla, B., Marcou, G., Belvisi, L., Nicotra, F., and Bernardi, A. (2007) First round of a focused library of cholera toxin inhibitors. *Carbohydr. Res. 342*, 1651–1660.

(33) Aldhoun, M., Massi, A., and Dondoni, A. (2008) Click azide-nitrile cycloaddition as a new ligation tool for the synthesis of tetrazole-tethered C-glycosyl α-amino acids. *J. Org. Chem. 73*, 9565–9575.

(34) Chan, W. C., and White, P. D. (2000) Basic procedures, in *Fmoc Solid Phase Peptide Synthesis: A Practical Approach* (Chan, W. C., and White, P. D., Eds.) pp 41–76, Oxford University Press, Oxford.

(35) Löber, S., Rodriguez-Loaiza, P., and Gmeiner, P. (2003) Click linker: efficient and high-yielding synthesis of a new family of SPOS resins by 1,3-dipolar cycloaddition. *Org. Lett. 5*, 1753–1755.

(36) Turner, R. A., Oliver, A. G., and Lokey, R. S. (2007) Click chemistry as a macrocyclization tool in the solid-phase synthesis of small cyclic peptides. *Org. Lett. 9*, 5011–5014.

(37) Gasser, G., Hüsken, N., Köster, S. D., and Metzler-Nolte, N. (2008) Synthesis of organometallic PNA oligomers by click chemistry. *Chem. Commun. 31*, 3675–3677.

(38) Singh, I., Vyle, J. S., and Heaney, F. (2009) Fast, copper-free click chemistry: a convenient solid-phase approach to oligonucleotide conjugation. *Chem. Commun. 32*, 3276–3278.

(39) Sharma, P., and Moses, J. E. (2010) Ethynyldiisopropylsilyl: a new alkynylsilane protecting group and "click" linker. *Org. Lett. 12*, 2860–2863.

(40) Santini, R., Griffith, M. C., and Qi, M. (1998) A measure of solvent effects on swelling of resins for solid phase organic synthesis. *Tetrahedron Lett. 39*, 8951–8954.

(41) Bock, V. D., Hiemstra, H., and van Maarseveen, J. H. (2006) Cu^I-catalyzed alkyne-azide "Click" cycloadditions from a mechanistic and synthetic perspective. *Eur. J. Org. Chem.* 51–68.

(42) Bouillon, C., Meyer, A., Vidal, S., Jochum, A., Chevolot, Y., Cloarec, J.-P., Praly, J.-P., Vasseur, J.-J., and Morvan, F. (2006) Microwave assisted "Click" chemistry for the synthesis of multiple labeled-carbohydrate oligonucleotides on solid support. *J. Org. Chem. 71* 4700–4702.

(43) Raymond, J. A., Radding, W., and DeVries, A. L. (1977) Circular dichroism of protein and glycoprotein fish antifreezes. *Biopolymers 16*, 2575–2578.

(44) Eniade, A., Purushotham, M., Ben, R., N., Wang, J. B., and Horwath, K. (2003) A serendipitous discovery of antifreeze protein-specific activity in C-linked antifreeze glycoprotein analogs. *Cell Biochem. Biophys. 38*, 115–124.